Colloid and Interface Science Communications 26 (2018) 24–31

Contents lists available at ScienceDirect

Colloid and Interface Science Communications

journal homepage: www.elsevier.com/locate/colcom

Effect of Xanthone and 1-Hydroxy Xanthone on the Dipole Potential of Lipid Membranes

J.P. Cejas[a], A.S. Rosa[a], H.A. Pérez[a], L. Alarcón[b], C. Menéndez[b], G.A. Appignanesi[b], A. Disalvo[a], M.A. Frías[a,*]

[a] Applied Biophysics and Food Research Center (Centro de Investigaciones en Biofisica Aplicada y Alimentos, CIBAAL, National University of Santiago del Estero and CONICET, RN 9 - Km 1125, 4206 Santiago del Estero, Argentina.
[b] INQUISUR, Dpto. de Química, Universidad Nacional del Sur (UNS)-CONICET, Av. Alem 1253, 8000 Bahía Blanca, Argentina

ARTICLE INFO

Keywords:
Lipid monolayers
Xanthones
1-OH Xanthone
Dipole potential
Carbonyl groups
Hydration

ABSTRACT

Xanthone (Xa) and 1-OH Xanthone (1-OHXa) in 1,2-dipalmitoyl-*sn*-glycero-3-phosphocholine (DPPC) membranes increase the dipole potential. Results with 1,2-di-O-tetradecyl-*sn*-glycero-3-phosphocholine (Ether PC), lacking carbonyl groups, indicate that the CO dipole of Xa molecule does not contribute to the increase of dipole potential. Molecular Dynamics calculations confirm that CO group of Xa locates parallel to the membrane interphase. Xa decreases the area per lipid in DPPC monolayers and the membrane polarity as measured by GP of Laurdan explaining the dipole potential increase. This rearrangement of water in the CO region is consistent with Fourier Transform Infrared Spectroscopy results indicating that CO of Xa are buried in the membrane phase. In contrast, CO groups of DPPC show an additional population of bound COs that seems to be more exposed to water, which contributes to the increase in dipole potential. These results are also corroborated by MD simulations.

1. Introduction

Xanthones are oxygenated heterocyclic compounds structurally typified by the presence of a dibenzo-γ-pirone system differing in the position and nature of the substituents [1]. Unsubstituted xanthones play an important role as pharmacophores. In turn, substituted xanthones or xanthen-9H-one derivatives are a class of compounds with high therapeutic potential [2].

There are over fifty natural xanthones extracted from *mangosteen* [3–6] among others. The taxonomic importance in xanthone families have aroused great interest not only for the chemosystematic investigation but also from the pharmacological point of view like antimalarial [7], antibacterial [8, 9], antifungal [10] [11], antioxidant, antitumoral [12, 13], antimicrobial and anti-hepatotoxic effects, as well as anti-inflammatory activity [14] and anti-Alzheimer properties [15–17]. Moreover, it is used in the preparation of xanthydrol for the determination of urea in blood and found in essential oils from genciana and other flowers and also isolated from pil in Norway coasts.

Xanthones are present in plants and their specific substituents can act [18] as defence compounds against herbivores and microorganisms. In this regard, it was introduced in the market as an insecticide, ovicida and larvicide for the butterfly *carpocapsa* [19–22].

This diversity of functions makes them interesting in regard to their specific effects on cellular structures. The structures of 9H-Xanthen-9-one (Xa) and 1-hydroxy-9H-xanthen-9-one (1-OHXa) (Fig. S1A and B) are well known by Infrared Spectroscopy, Mass Spectral and Nuclear Magnetic Resonance data [23]. Xanthone skeleton has a hydrophobic core composed of a heterocycle of xanthene oxidized in position 9 and a carbonyl group (Fig. S1A). On the other hand, 1-OHXa (Fig. S1B) shows a certain degree of hydrophylicity due to the presence of an −OH group in position 1.

The molecular features of Xa make it insoluble in water and highly soluble in organic solvents. Hence, due to its non-polar character, it is expected that at least some of its biological effects would take place affecting membrane properties. In this regard, effects of hydroxy-xanthones on the physicochemical properties of dipalmitoylphosphatidylcholine (DPPC) liposomes have been investigated in terms of lipid bilayer phase state, by means of molecular dynamics simulations and surface properties such as, zeta potential studies. In this direction, recently it has been reported that the entrapment of xanthones in

Abbreviations: DPPC, 1,2-dipalmitoyl-*sn*-glycero-3-phosphocholine; DOPC, 1,2-dioleoyl-*sn*-glycero-3-phosphocholine; EtherPC, 1,2-di-O-tetradecyl-*sn*-glycero-3-phosphocholine; Xa, 9H-Xanthen-9-one; 1-OHXa, 1-hydroxy-9H-Xanthen-9-one.

* Corresponding author.
E-mail address: marafrias@hotmail.com (M.A. Frías).

https://doi.org/10.1016/j.colcom.2018.08.001
Received 18 June 2018; Received in revised form 30 July 2018; Accepted 1 August 2018

biomimetic systems such as liposomes can enhance its absorption through the biological membranes [24].

Xanthene dyes, such as fluorescein, rose bengal B, erythrosine B and eosin Y, have been found to affect the dipole potential of membranes composed of diphytanoylphosphocholine, diphytanoylphosphoserine, and diphytanoylphosphoethanolamine. Adsorption of Rose Bengal on the bilayer interface leads to a reduction of the dipole potential drop at the membrane-solution boundary. The effect was ascribed to their uncharged and charged forms, respectively. In the case of the xanthene dye fluorescein, it was shown that it remains on one side of the BLM, revealing a low partition in the membrane phase and that its action is mainly produced at the interphase [25–27].

However, xanthones localization within the membrane and its effects on the organization of the lipid membrane surface, are not yet clear. Since surface properties, in particular dipole potential, are determinant for adsorption and absorption of peptides and proteins and in adhesion phenomena, it is important to know how these compounds may affect those properties in lipid membrane.

Therefore, the aim of this work is to determine the possible mechanism of Xa to change the surface properties of lipid interphases, considering that these are determinant in adhesion, partition and fusion processes. In particular, the effect of 9H-Xanthen-9-one (Xa) and 1-hydroxy-9H-Xanthen-9-one (1-OHXa) on dipole potential, molecular packing and hydration of lipid membranes was carried out by fluorescent spectroscopy, FTIR and Molecular Dynamics simulations.

2. Materials and Methods

2.1. Lipids and Chemicals

Chemicals: 1,2-dipalmitoyl-*sn*-glycero-3-phosphocholine (DPPC); 1,2-dioleoyl-*sn*-glycero-3-phosphocholine (DOPC); 1,2-di-O-tetradecyl-*sn*-glycero-3-phosphocholine (Ether PC) were purchased from Avanti Polar Lipids Inc. (Alabaster, AL). 9H-Xanthen-9-one (Xa) (MW: 196.19 g/mol) was from Sigma-Aldrich. Purity of lipids and xanthones were higher than > 99% as checked by FTIR and UV spectroscopies. Laurdan (6-dodecanoyl-2-dimethyl aminonaphthalene) was obtained from Molecular Probes and used without further purification. 1-hydroxy-9H-xanthen-9-one (1-OHXa) (MW: 212.20 g/mol) was synthesized from Xa following the protocol of Grover, Shah, Shah (GSS) [28] by reacting equimolecular mixtures of salicylic acid and resorcinol in the presence of zinc chloride at 170 °C for 6 h. Purification was performed by column chromatography using silica gel as adsorbent and hexane/AcOEt as eluent. Partition coefficient experimental values (log P) for Xa base and 1OHXa were determined by applying the ampoule method (Shake-Flask) at room temperature (25 °C) using *n*-octanol as a non-polar phase at pH = 7.4.

2.2. Surface Pressure – Molecular Area (π- A) Isotherms

Surface pressure – molecular area (π- A) isotherms were carried out in a KSV NIMA LB trough (surface area = 240.00 cm^2) using a Pt Wilhelmy plate (39.24 mm^2) as sensor. Accurate volumes of lipids dissolved in chloroform were spread on the surface of 1 mM KCl aqueous solution (pH 5), using a Hamilton micro syringe with an error within ± 0.01 mL. The Platinum probe was flamed until glowed red-hot before each assay. The trough was filled with the barriers in a fully open position. An appropriate volume was added checking that the borders of the meniscus were even in the whole perimeter. Monolayers were allowed to stabilize during 10 min before each measurements. The whole equipment was enclosed in an acrylic box to minimize water evaporation and to avoid contaminations from the environment during the study. Compression curves were carried out at a constant speed (5 mm/min) at 20 ± 2 °C. Data correspond to an average of at least three experimental runs for each lipid Xa or 1-OHXa ratio.

2.3. Dipole Potential Measurements

Dipole potential (ψ_D) was determined in monolayers formed on an air–water interface of a 1 mM KCl aqueous solution by spreading chloroform solutions of each lipid/Xa or 1-OHXa mixture. Data correspond to an average of at least three experimental runs for each mixture. Different aliquots of each mixture were added until constant surface pressure was achieved [29, 30]. In this condition, the interfacial potential was determined through a circuit of high impedance, connecting a vibrating electrode above the monolayer and a reference Ag/AgCl electrode in the aqueous subphase. The temperature was set at 20 ± 0.5 °C controlled with a calibrated thermocouple immersed in the subphase. Therefore, the reference potential is constant at the temperature of measurement [31].

2.4. ATR-FTIR Spectroscopy

All ATR-FTIR spectra were obtained in a Thermo Scientific 6700 spectrometer with DTGS detector, connected to a system of circulation of dry air to avoid the interference of water vapor and carbon dioxide. The molar ratio of lipid/Xa and lipid/1-OHXa in each film was 70:30. The films were prepared by evaporating the chloroform solvent. Then, they were resuspended in a minimum volume of MQ water at 5 pH. Droplet (50 μL) of each suspension was placed on ZnSe crystal (45° incident angle). Samples were allowed to stabilize at 25 °C and a relative humidity of 35% before each measurement. Spectra were obtained with intervals of three minutes in order to control the water content evolution following the water band intensity and the asymmetric stretching vibration of the methylene groups. Data were obtained after 64 scans per sample at a 4 cm^{-1} resolution and were the average of three independent assays. Spectra were analysed with a Microcal Origin program (version 8.5) applying a combination of Fourier deconvolution and curve-fitting procedures to reconstruct the contours of the original band envelope [32, 33].

2.5. Molecular Dynamics Simulations

Molecular dynamics simulations of DPPC bilayers were performed using AMBER12 simulation package [34] and Lipid11 force field [35]. Initially, the bilayer was composed of 128 DPPC molecules (64 per monolayer in an 8 × 8 arrangement) with a separation between DPPC molecules of 9 Å in a square arrangement. Nine DPPC molecules for each monolayer in alternate places were removed and xanthones were added in the generated free spaces. The membrane was stabilized at $T = 293$ K and solvated with 10,640 TIP3P water molecules [36, 37] (which means around 83 water molecules per lipid) in order to assure that the system was fully hydrated. Solvation was done along the Z axis and the system was subjected to periodic boundary conditions along the (X,Y) plane. The minimization was carried out in two steps, both at constant volume. In the first step solvent were minimized keeping fixed the atoms of the membrane and xanthones, and then releasing it to minimize the entire system. The equilibration of the dimensions and density of the system was achieved after stabilizing the system temperature using the Langevin thermostat [38] and keeping fixed the bilayer. Then, all restraints were removed and the bilayer was free to establish a lipid-lipid equilibrium distance. After 300 ns equilibration, the area per lipid was consistent with experimental values. Both equilibration and final production data used a NPT assembly, with the SHAKE activated for hydrogen bonds, with 10 Å interaction cut off. Production runs typically elapsed 500 ps, but we also performed some larger runs to test the consistency of our results.

2.6. Generalized Polarization with Laurdan

Fluorescence measurements were carried out in a SLM 4800 spectrofluorometer. Multilamellar vesicles (MLV's) were prepared for the

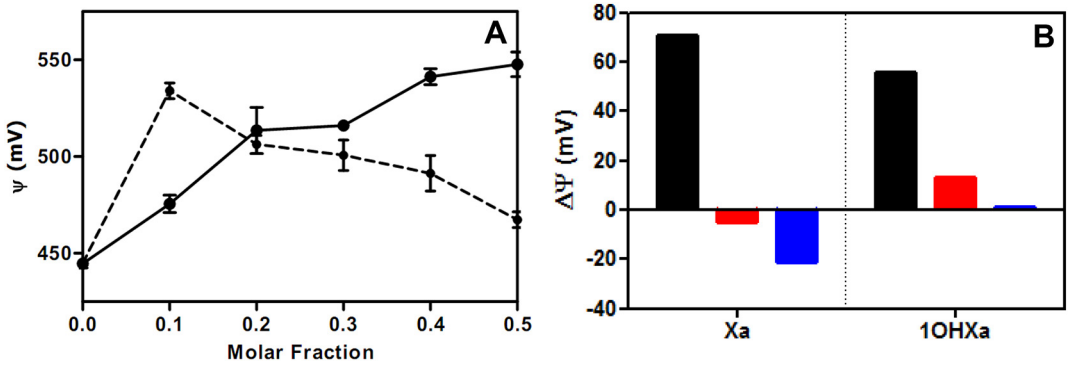

Fig. 1. A) Dipole potential of monolayers with different DPPC/Xa (black full line) and DPPC/1-OHXa (dashed black line) molar ratio spread on 1 mM KCl subphase at 22° C. B) Differential changes of dipole potential in the presence of Xa and 1-OHXa in DPPC (black bars); Ether PC (red bars) and DOPC (blue bars) monolayers at 22 °C. (For interpretation of the references to colour in this figure legend, the reader is referred to the web version of this article.)

relations 90:10, 80:20 and 70:30 lipid/Xa or lipid/1-OHXa. In all cases a Laurdan/lipid ratio of 1:300 was used. Laurdan concentration of the solutions was determined by absorption spectrophotometry in the ultraviolet region, at a maximum wavelength of 364 nm corresponding to an absorptivity coefficient of 20.000 M^{-1} cm^{-1}. Samples were stabilized every 5 °C in the range of 25 and 60 °C to determine the transition temperature [39, 40]. At each temperature the emission spectrum was obtained with a spectral scan from 400 to 600 nm with fixed excitation wavelength at 370 nm. The excitation spectra were obtained with a spectral scan from 300 to 430 nm with fixed gathering the fluorescence at 440 nm. From these spectra the generalized polarization (GP) corresponding to the emission and the excitation were calculated. These parameters were calculated as previously described by Parasassi et al. [40–42].

Table 1
Dipole Potential, Area per molecule and Dipole Potential per unit area for different lipid 70:30 lipid/Xa and lipid/1-OHXa mixtures.

Mixture	Dipole potential (mV)	Area per lipid ($Å^2$)	Dipole potential per unit area (mV/$Å^2$)
DPPC	445 ± 2	46.24	9.62
DPPC Xa	516 ± 2	43.74	11.80
DPPC 1-OHXa	501 ± 2	44.26	11.32
Ether PC	311 ± 4	48.11	6.46
Ether PC Xa	306 ± 6	45.28	6.76
Ether PC 1-OHXa	324 ± 9	50.86	6.37
DOPC	406 ± 4	49.21	8.25
DOPC Xa	385 ± 9	49.64	7.76
DOPC 1-OHXa	407 ± 13	51.84	7.85

3. Results

The dipole potential (ψ_D) of DPPC monolayers spread on an air/aqueous solution interphase increases monotonically with Xa concentrations to stabilize at 0.5 M fraction around 100 mV higher than pure DPPC monolayers (Fig. 1A). On the other hand, 1-OHXa gives a pronounced increase at 0.1 M fraction and decreases at higher ones.

The analysis of the effects of 1-OHXa on DPPC dipole potential can be done in three different ranges of concentrations. At 0.1 M fraction 1-OHXa increases the dipole potential in a rate similar as that found for Xa 0.5 M fraction. At 0.2 M fraction the dipole potential is similar for DPPC/Xa and DPPC/1-OHXa. At concentrations higher than 0.1 M fraction dipole potential decreases gradually and at 0.5 M fraction the effect of 1-OHXa is very small in comparison to Xa.

One important contribution to the dipole potential of a monolayer is the increase in the number of constitutive dipoles per unit area [43]. As inferred from the molecular structures in Fig. S1, both compounds Xa and 1-OHXa have carbonyl groups (CO) and 1-OHXa has, in addition, an −OH group, which dipole moments may contribute to the dipole potential of the membrane according to its orientation when inserted in the lipid interphase.

However, Fig. 1B shows that Xa does not affect the dipole potential of Ether PC at least in a PC:Xa ratio of 70:30 (red bar). Then, the possibility that the carbonyl group of Xa would be responsible of the dipole potential increase should be discarded. The slight increase produced by 1-OHXa ($\Delta\Psi = +13$), might be ascribed to the −OH in position 1 but this increase is much lower than in DPPC.

In the same Figure, the influence of both xanthones on the dipole potential of unsaturated DOPC is also shown (blue bars). Xa produces a decrease in the dipole potential of DOPC at the 30% ratio of about 20 mV with respect to the pure lipid.

Another property that can affect dipole potential is the area per lipid. The differential area per lipid values for the different mixtures are shown in Table 1 together with the dipole potential per unit area. These were obtained from compressibility modulus (C^{-1}) of mixtures of DPPC, DOPC and Ether PC with both compounds as shown in Supplementary material (Fig. S2).

The area changes produced by Xa in DPPC and in DOPC are congruent with the respective increase and decrease of dipole potential shown in Fig. 1.

Since dipole potential is also affected by water polarized in the carbonyl groups, the hydration of these groups in Xa and 1-OHXa mixtures with Ether PC groups is analysed by FTIR spectroscopy. As shown in Fig. 2A, the peak of the carbonyl group of Xa exposed to 35% RH is positioned at 1656.7 cm^{-1} and shifts slightly to higher frequencies in the presence of Ether PC. In addition, the shape of the curve changes and a shoulder that is not present in the pure Xa spectrum appears at higher frequencies. In contrast, the presence of a hydroxyl group in the ring causes a shift of the carbonyl stretching frequency of 1-OHXa to lower frequencies in the presence of Ether PC (1647.2 cm^{-1}) (Fig. 2B). It is concluded that CO group of Xa in Ether PC is buried in the membrane and thus less exposed to water vapor phase. On the contrary, CO of the 1-OHXa is more exposed to water which would explain the increase in the dipole potential as shown in Fig. 1B.

Thus, the effect of Xa on PC membrane dipole potential is not produced by the insertion of CO dipoles and appears strongly dependent on the lipid phase state since it increases in the condensed phase and decreases in the expanded one.

The orientation of Xa determined by molecular simulations is analysed in Fig. 3A. In gray, the density profiles of xanthones present in the system (specifically their centers of mass) are shown, as well as phosphate groups (red line), carbonyl groups (green line) and water molecules (blue line). It is observed that Xa is below the average values of density corresponding to the carbonyl groups and of the plane corresponding to water molecules more deeply stabilized in the membrane.

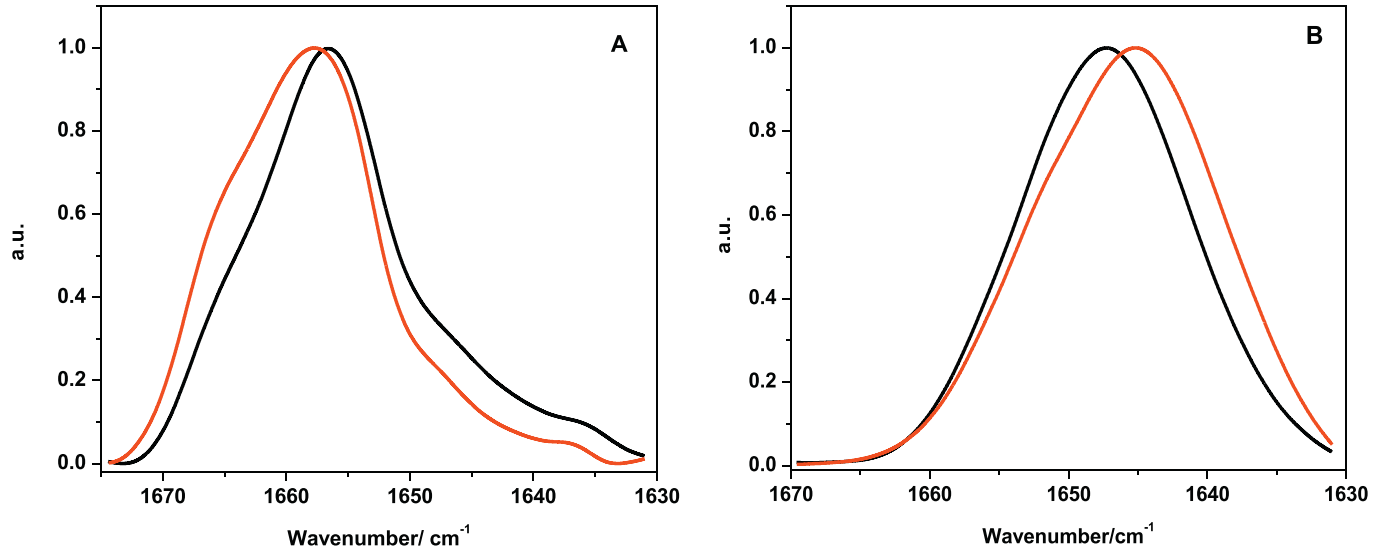

Fig. 2. A) Spectra of pure Xa (black line) and Xa in Ether PC in a 70:30 M ratio (red line) at 22 °C and RH: 35%. B) Spectra of pure 1-OHXa (black line) and 1-OHXa in Ether PC (red line) at 22 °C and RH: 35%. (For interpretation of the references to colour in this figure legend, the reader is referred to the web version of this article.)

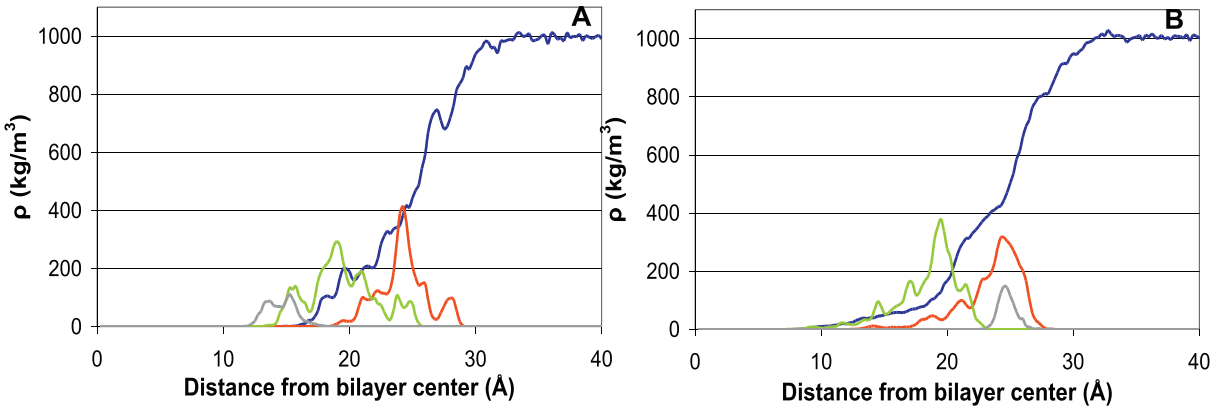

Fig. 3. A) Membrane density profiles of DPPC, Xanthone (skeleton Xa) and water for t = 500 ps. T = 293 K. Blue line corresponds to water; red line: phosphate groups; green line: carbonyl groups and gray line: Xa. B) Membrane density profiles of DPPC, 1-OHXa and water for t = 500 ps. T = 293 K. Blue line corresponds to water; red line: phosphate groups; green line: carbonyl groups and gray line: 1-OHXa. (For interpretation of the references to colour in this figure legend, the reader is referred to the web version of this article.)

Different significant results for 1-OHXa were obtained by MD (Fig. 3B). In this Figure, it is observed that 1-OHXa stabilizes well above the carbonyl region in between the phosphate groups where water can be found. The orientations of the Xa molecules with respect to the surface were calculated to know not only their positions with respect to the DPPC molecules but also how they are arranged in the membrane (Fig. S3). The carbon-oxygen bond angles of the carbonyl group located in the central ring of Xa with respect to the normal to the surface of the DPPC membrane were calculated. For a time interval of 500 ps, Xa has a preferential orientation forming an angle between 90 and 135° with respect to the normal to the surface. Similar results were obtained for longer times. Taking together, the orientation of Xa and 1-OHXa with respect to the acyl chains are similar although at different depths. Thus, MD results confirm that the increase in dipole potential cannot be explained by insertions of Xa CO dipoles normal to the interphase plane.

One contribution to dipole potential, in addition to the alignments of the constitutive dipoles is water polarized at the interphase. The changes in polarity have been ascribed to the number and motional freedom of the water molecules in the membrane phase [44–46] and related to generalized polarization (GP) values of the Laurdan fluorescent. This probe is located at the level of sn-1 carbonyl of the phospholipids inside the bilayer [47], being able to “sense” changes in the interface region between the hydrophobic core and the external hydrophilic bulk. The transition dipole of Laurdan (4.4–5.0 D) [48] enables a large bathochromic shift of the excitation and emission spectra in solvents with different polarity.

This sensitivity to environment polarity makes Laurdan very useful in evaluating the hydration of lipid bilayer interfaces.

The presence of Xa and 1-OHXa does not affect significantly the transition temperature of DPPC (Fig. S4A) at 70:30 M ratio. The second derivatives of curves in part A are plotted as a function of temperature in Fig. S4B. Similar results were obtained with etherPC (data not shown).

The transition temperature of DPPC at different Xa and 1-OHXa molar ratios were determined by following the GP emission and GP excitation with temperature, as it was previously reported [39, 40, 44, 45]. The transition temperature of DPPC measured by GP decreases with Xa concentration in the same trend as reported by Zeta Potential and DSC measurements [24]. In this work, it is shown that Xa and 1-OHXa displace and make the pre-transition temperature disappear. There are no studies regarding this effect. In our case, GP measurements do not detect the pre-transition temperature. However, the effect on hydration is clearly discussed considering fluorescence measurements. GP values calculated from the emission spectra are not changed by Xa

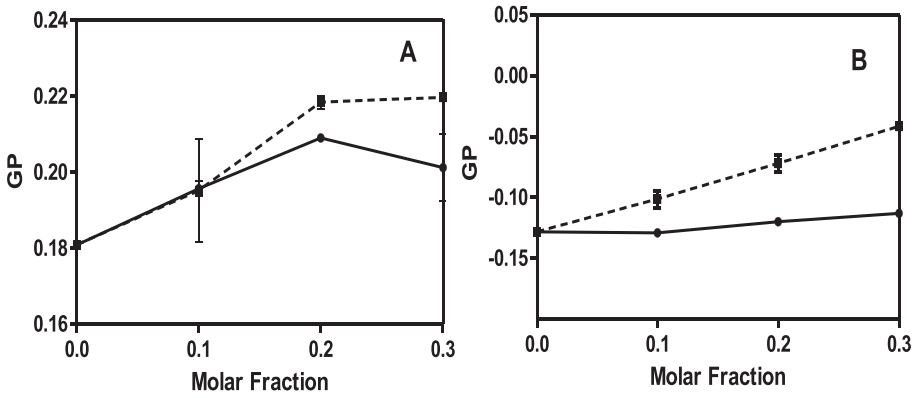

Fig. 4. A) GP values of DPPC doped with fluorescent probe Laurdan at different ratios of Xa (solid black line) and 1-OHXa (dash black line) at 25 °C. B) GP values of DPPC doped with fluorescent probe Laurdan at different ratios of Xa (solid black line) and 1-OHXa (dash black line) at 50 °C.

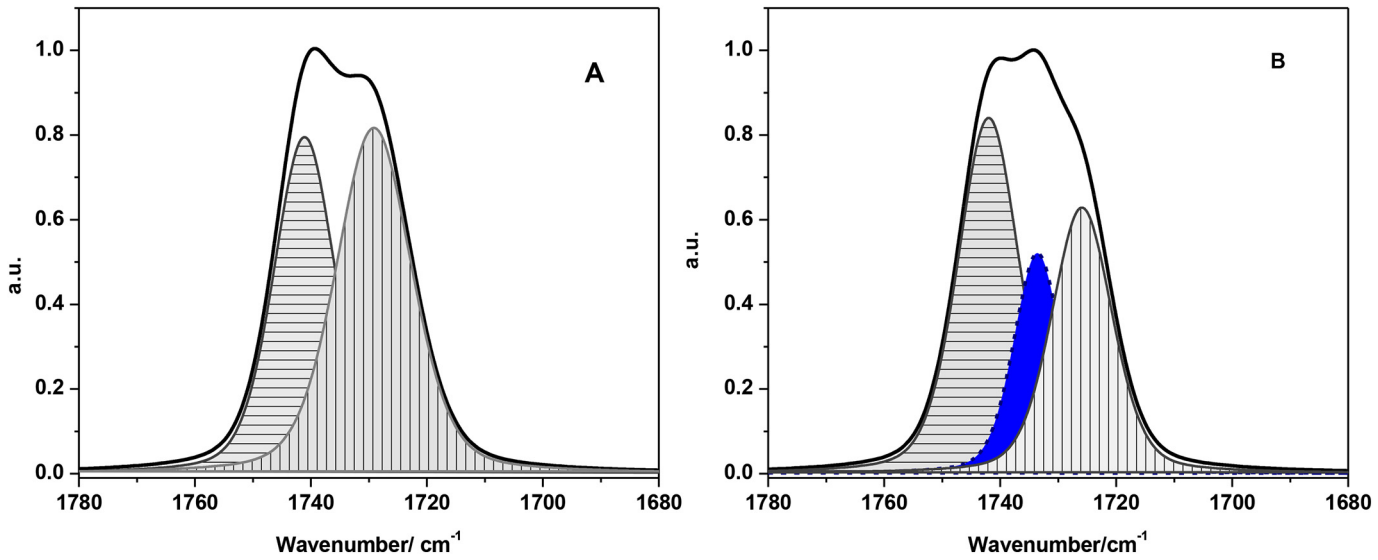

Fig. 5. FTIR spectra of DPPC Xa and 1-OHXa in the region of carbonyl groups. A) Pure DPPC; B) DPPC: Xa (70:30 ratio) at 25 °C and RH 35%.

and 1-OHXa phase state up to 0.3 M fraction of DPPC bilayers (Fig. S4A).

However, when calculated from excitation spectrum both compounds increase the GP values (Fig. S4C). This is better observed in Fig. 4A and B where it is shown also that only 1-OHXa affects the liquid crystalline state. A dependence of the GP on the excitation wavelength, measured at fixed emission wavelengths, is an indication that more than one phase is present because the excitation spectrum of Laurdan is different in the gel and liquid crystalline phases [40].

If this is so, Xa and 1-OHXa may affect hydration layers causing a change in the dipole potential due to a partial condensation of the interphase. GP variation with concentration indicates that Xa and 1-OHXa decrease the polarity of the interphase in the gel phase congruent with the area decrease. These changes may affect the dielectric properties of the lipid membranes as it was reported [49]. It has been also shown that water may penetrate the lipid bilayer reaching a plane located at the region of the carbonyl groups [49–51].

The density profiles of Fig. 4A denote that Xa locates below the region of the CO groups of the phospholipids. Thus, Xa may be affecting the hydration properties of the CO phospholipid groups.

The method that provides a visualization of the membrane state at the molecular level, both of lipids and water without adding perturbing probes is FTIR spectroscopy. ATR/FTIR analysis of the carbonyl groups in Fig. 5 depicts the profiles of frequency shifts of bound and unbound carbonyl groups. Deconvolution and curve fitting were performed to determine the position and relative contribution of the two carbonyl group populations. Spectra of $\nu_{C=O}$ region show the contribution of two populations. One of them corresponds to the unbound population centered at 1741 cm^{-1} (height = 0.796; %Area = 44) and the other to the H-bound conformers centered at 1729 cm^{-1} (height = 0.817; %Area = 56) for pure DPPC [52, 53] (Fig. 5A).

In the presence of Xa (Fig. 5B), the unbound population band for pure DPPC remains unchanged (1742 cm^{-1}; height = 0.824; %Area = 43) while the hydrated population (H-bound) splits in two bands one at 1726 cm^{-1} (height = 0.652; %Area = 35) and the other at 1733 cm^{-1} (height = 0.503; %Area = 22). These two new bands have different intensities and area under the peak.

The appearance of a new peak at lower frequencies suggests that part of the H-bound population of C=O would orient in a lower angle with respect to the normal to the surface and therefore more exposed to water, which would explain the increase in dipole potential.

In contrast, spectra of DPPC:1-OHXa show no effects on carbonyl group populations in comparison to the control of pure DPPC (Fig. S5).

In Ether PC bilayers, methyl and methylene groups do not experience changes in their vibrational frequencies in the presence of Xa or 1-OHXa. The symmetric phosphate groups are not affected either by the presence of Xa or 1-OHXa. Thus, the unique centre of hydration that is affected by Xa are the CO groups.

According to the density profiles shown above, Xa locates below the region of the CO groups of the phospholipids. This insertion

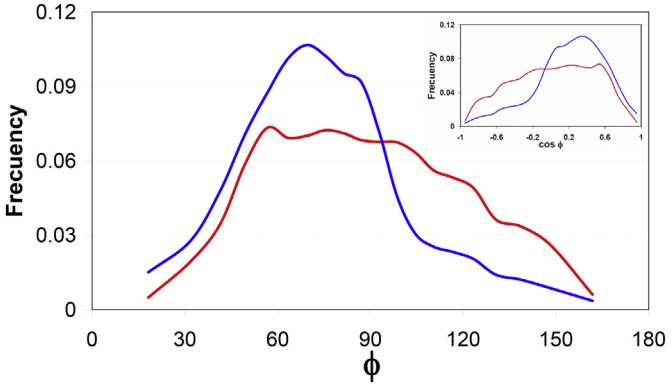

Fig. 6. Orientation of the water hydrogen bound lipid carbonyls (CO) with respect to the normal to the membrane surface. Pure DPPC (red line) and DPPC/Xa (blue line) at T = 293 K. T293x27 indicates a membrane with 27 Xa molecules incorporated to the membrane. (For interpretation of the references to colour in this figure legend, the reader is referred to the web version of this article.)

modifies their hydration properties as shown by GP of Laurdan and FTIR spectra.

MD calculations indicate that the presence of Xa modifies the quality of the H bonds linked to the CO groups (Fig. 6). The angles of the CO groups in pure DPPC (red curve) are between 50 and 90 degrees. In the presence of Xa (blue curve) the region of small angles increases i.e. the CO group aligned with the normal to the surface increases generating a defined peak at 65 degrees. This is consistent with the contribution of the CO to dipole potential increase.

4. Discussion

The contributions to the dipole potential of the CO groups of Xa is disregarded since no effect of Xa are found in Ether PC since, according to FTIR results they are buried in the membrane phase and hence weakly hydrated. Instead, the results show clearly that Xa increases the dipole potential of DPPC membranes in the condensed state at 30% mol/mol ratio by affecting the orientation of the phospholipids CO groups and reorganizing their hydration shell.

This effect of Xa on membrane surface potential is dependent on the molecular structure of Xa and of the phospholipid chain.

The presence of OH, as it was the case of 1-OHXa, does not affect the CO phospholipids groups and the increase in dipole potential can be ascribed to the orientation of the OH group. Since it was demonstrated by FTIR spectroscopy that 1-OHXa does not affect the population of the carbonyl groups (CO) (Fig. S5), the different effects of this compound on dipole potential as described above can be ascribed to differences in its orientation at different concentrations with respect to the membrane interphase. The observation that 1-OHXa increases the dipole potential of 1,2-di-O-tetradecyl-*sn*-glycero-3-phosphocholine (Ether PC) could be explained by the orientation of the −OH group at the membrane interphase. MD simulation results report that this derivative stabilizes in a region well above the carbonyl groups near the phosphates ones. Thus, the CO groups of 1-OHXa are more exposed to water according to the frequency shift observed in Fig. 2 and Fig. S3. This may be due to the fact that the CO and OH proximity in 1-OHXa, constitute a hydrophilic region that stabilizes the molecule in the outer polar region of the membrane. Furthermore, at low concentrations these groups would contribute to the increase in dipole potential. At increasing concentrations, it will rotate towards the membrane interior orienting the CO and the OH into the interphase decreasing gradually the dipole potential as shown in Fig. 1A. In addition, 1-OHXa displays an increase in GP in the fluid phase (Fig. 4B) which can be explained considering that with concentration increase the molecule orients with the skeleton parallel to the acyl chain in a similar way as cholesterol does [40, 54]. This is congruent with the null effect on the dipole potential and the dehydration effect.

In regard to the phospholipid chain the dipole potential per unit area of DOPC/Xa decreases (see Table 1). This is a concurrent effect of a slight area increase and the decrease of the total dipole potential. There is no evidence of an effect of Xa on the carbonyl group orientation as observed in DPPC (FTIR data not shown). The insertion of the Xa skeleton would expand the area per lipid opposing its dipole residues to the phospholipid CO dipoles.

Molecular dynamics results indicate that both Xa and 1-OHXa insert with the skeleton normal to the membrane surface plane leaving the CO groups parallel to it and therefore with null contribution to the dipole potential.

The frequency band of Xa carbonyl groups shows modifications in the presence of Ether PC. It is observed that the frequency is displaced to higher frequencies suggesting that the CO exposure to water is reduced when inserted in the lipid membrane. This would account for a weaker interaction in comparison to the H-bonds with water. The decrease in area would indicate a short distance interaction.

The observation that 1-OHXa increases the dipole potential of Ether PC could be explained by the orientation of the −OH group at the membrane interphase (Fig. 2). This is congruent with the results of MD reporting that these derivative stabilizes in a region above the carbonyl group. In this case, the CO groups of 1-OHXa is more exposed to water according to the frequency shift observed in Fig. 2 and Fig. S3.

In consequence, a possibility that may explain the dipole potential increase when Xa is inserted in that position is that the molecule affects the distribution and orientation of the phospholipid carbonyl groups by changing in some extent the packing of the interphase and its hydration.

The area decrease would indicate a reorganization of the hydration layer around the polar head groups or in the adjacent CH_2. FTIR results show that the only hydration centre affected by Xa insertion are the carbonyl groups of the phospholipids.

The reorientation of the CO groups is reflected by the changes in surface polarization with Laurdan. This seems to be supported by the analysis of the splitting of the carbonyl group bands obtained by ATR/FTIR analysis. Although the unbound population (band centred at the higher frequency) is not altered, the significant split of the H-bound population into a band at 1735 cm^{-1} (22%) and at 1724 cm^{-1} (35%) indicates that there is a 0.63 fraction of the H-bound population which is more exposed to water.

Considering that the dipole potential is given by Eq. 1:

$$\Psi = \Psi_0 \cos\theta \quad (1)$$

where Ψ_0 is the dipole potential corresponding to that obtained when all dipoles in the system are oriented normal to the membrane surface.

Introducing a value of $\theta_L = 63^\circ$ for the angle corresponding to carbonyl groups in pure DPPC [55] the angle for the same groups in the presence of Xa can be calculated by Eq. 2:

$$\Psi_{Xa} = (\Psi_L \mid \cos 63).\ \cos\theta_{Xa} \quad (2)$$

When the experimental values for dipole potential of Xa mixtures $\Psi_{xa} = 510$ mV and pure lipids $\Psi_L = 448$ mV are introduced, $\theta_x = 58^\circ$.

That is, a tilt in 5° towards the interphase produces an increase of 62 mV in dipole potential. In addition, this reorientation may be a consequence of the packing increase produce by Xa (Fig. 2) which in turn may produce water reorganization. This is schematically described in Fig. 7.

The changes in the H-bound carbonyl group population is congruent with the changes in hydration observed with Laurdan. The effect of Xa on the compressibility and area takes place with a decrease in hydration and polarity of the interphase in accordance with GP values.

Considering that the 55% (area under the curve) of H-bound CO of DPPC is split in two populations, respectively, the fractions of H-bound

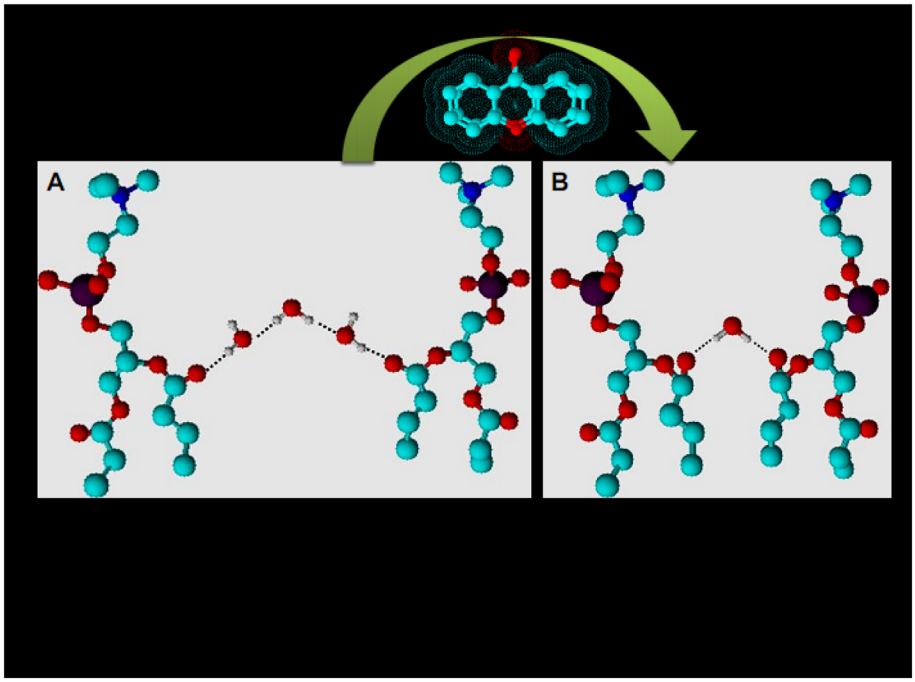

Fig. 7. Schematic diagram of the reorientation of DPPC carbonyl groups by Xa insertion. Note effects of water molecules on the carbonyl region.

populations corresponding to those carbonyls shifted to lower frequencies i. e more exposed to water is 0.6 and the rest is in a position similar to pure PC.

Thus, the dipole potential with Xa corresponding to perturbed and non perturbed carbonyl groups is

$\Psi_{xa} = 0.60 \times 995.5\,mV \times \cos \quad 58 + 0.40 \times 995.5 \times \cos \quad 63 = 496\,mV$.which is quite comparable to the experimental value of 510 mV. The difference might be ascribed to other contributions to the dipole potential, concomitant with CO reorientation.

The scheme in Fig. 7 resumes all changes that would take place in the membrane interphase by insertion of Xa. In part A, the carbonyl group of the pure lipids is tilted with respect to the normal in 63°. In this condition, the organization of water to link to adjacent carbonyl groups respecting the orientation of the H bonds involves 4 water molecules with a given area and with loose packing. In the presence of Xa (part B), packing increases, CO groups orient normal to the surface (decreasing the angle to 58°), reducing the area and the compressibility with a lower amount of water molecules as observed with Laurdan, all of them contributing to the dipole potential increase.

On the other hand, 1-OHXa does not affect the CO orientation as seen by FTIR/ATR congruent to MD results. In this case the effect on area and compressibility is comparable to that observed with Xa skeleton but the dipole potential increases in Ether PC. Thus, the dipole potential increase can be explained considering that the OH group of 1-OHXa is oriented in the surface, because, as shown by MD, this compound stabilizes in the phosphate region without affecting the carbonyl groups of the lipid. In addition, it also shows an increase in GP at 25 °C indicating a partial water rearrangement.

5. Conclusion

The mechanism of the increase in membrane dipole potential of ester lipids mediated by xanthone and 1-hydroxy xanthone was examined utilizing fluorescence, FTIR and molecular dynamics simulations. It is concluded that rearrangement of water molecules in the membrane interfacial region (rich in carbonyls) contributes to the increase in dipole potential.

As the dipole potential reflects the image charge of the membrane interior being this positive and the hydration forces, the increase in dipole potential would favor the insertion of negatively charged effectors and disfavor those positively charged. In addition, it could be important to consider the contribution of the hydration in membrane-membrane or membrane-peptides interactions.

This work is a necessary stage previous to the analysis of more complex systems in mixed membranes where domains might be present.

Supplementary data to this article can be found online at https://doi.org/10.1016/j.colcom.2018.08.001.

Acknowledgements

This work was supported with funds from CONICET (PIP 0484 and 11220150100393CO), UNSE (23/A164), PGI-UNS 24/Q062, and ANPCyT (PICT 2015-1111, PICT 2012-2602 and PICT 2010-119, PICT 2015-1893). EAD, GAA, LMA, MAF are members of the research career of CONICET, RA. JPC, ASR and CM are recipients of a fellowship from CONICET, RA. HAP is recipients of a fellowship from ANPCyT-MINCyT, RA.

References

[1] N. Chairungsrilerd, K. Takeuchi, Y. Ohizumi, S. Nozoe, T. Ohta, Mangostanol, a prenyl xanthone from Garcinia mangostana, Phytochemistry 43 (1996) 1099–1102.
[2] M. Markiewicz, T. Librowski, A. Lipkowska, P. Serda, K. Baczynski, M. Pasenkiewicz-Gierula, Assessing gastric toxicity of xanthone derivatives of anti-inflammatory activity using simulation and experimental approaches, Biophys. Chem. 220 (2017) 20–33.
[3] J. Pedraza-Chaverri, N. Cárdenas-Rodríguez, M. Orozco-Ibarra, J.M. Pérez-Rojas, Medicinal properties of mangosteen (Garcinia mangostana), Food Chem. Toxicol. 46 (2008) 3227–3239.
[4] K. Matsumoto, Y. Akao, E. Kobayashi, K. Ohguchi, T. Ito, T. Tanaka, M. Iinuma, Y. Nozawa, Induction of apoptosis by xanthones from mangosteen in human leukemia cell lines, J. Nat. Prod. 66 (2003) 1124–1127.
[5] K. Matsumoto, Y. Akao, H. Yi, K. Ohguchi, T. Ito, T. Tanaka, E. Kobayashi, M. Iinuma, Y. Nozawa, Preferential target is mitochondria in α-mangostin-induced apoptosis in human leukemia HL60 cells, Bioorg. Med. Chem. 12 (2004) 5799–5806.

[6] M. Pedro, F. Cerqueira, M.E. Sousa, M.S.J. Nascimento, M. Pinto, Xanthones as inhibitors of growth of human cancer cell lines and their effects on the proliferation of human lymphocytes in vitro, Bioorg. Med. Chem. 10 (2002) 3725–3730.
[7] W. Mahabusarakam, K. Kuaha, P. Wilairat, W.C. Taylor, Prenylated xanthones as potential antiplasmodial substances, Planta Med. 72 (2006) 912–916.
[8] S. Laphookhieo, J.K. Syers, R. Kiattansakul, K. Chantrapromma, Cytotoxic and antimalarial prenylated xanthones from Cratoxylum cochinchinense, Chem. Pharm. Bull. 54 (2006) 745–747.
[9] S. Rassameemasmaung, A. Sirikulsathean, C. Amornchat, K. Hirunrat, P. Rojanapanthu, W. Gritsanapan, Effects of herbal mouthwash containing the pericarp extract of Garcinia mangostana L on halitosis, plaque and papillary bleeding index, J. Int. Acad. Periodontol. 9 (2007) 19–25.
[10] C.B. de Koning, R.G. Giles, L.M. Engelhardt, A.H. Whitet, Convenient syntheses of the naturally occurring benzo [b] xanthen-12-one bikaverin. X-Ray crystallographic confirmation of the product regiochemistry, J. Chem. Soc. Perkin Trans. 1 (1988) 3209–3216.
[11] M. Pickert, K.J. Schaper, A.W. Frahm, Substituted xanthones as antimycobacterial agents, part 2: antimycobacterial activity, Arch. Pharm. 331 (1998) 193–197.
[12] A. Groweiss, J.H. Cardellina, M.R. Boyd, HIV-inhibitory prenylated xanthones and flavones from Maclura t inctoria 1, J. Nat. Prod. 63 (2000) 1537–1539.
[13] A. Zarena, K.U. Sankar, Screening of xanthone from mangosteen (Garcinia mangostana L.) peels and their effect on cytochrome c reductase and phosphomolybdenum activity, J. Nat. Prod. India 2 (2009) 23–30.
[14] T. Librowski, R. Czamecki, M. Jastrzebska, Chiral 2-amino-1-butanol xanthone derivatives as potential antiarrhythmic and hypotensive agents, Acta Pol. Pharm. 56 (1999) 87–90.
[15] H.R. El-Seedi, M. El-Barbary, D. El-Ghorab, L. Bohlin, A.-K. Borg-Karlson, U. Goransson, R. Verpoorte, Recent insights into the biosynthesis and biological activities of natural xanthones, Curr. Med. Chem. 17 (2010) 854–901.
[16] S.-n. Wang, Q. Li, M.-h. Jing, E. Alba, X.-h. Yang, R. Sabaté, Y.-f. Han, R.-b. Pi, W.-j. Lan, X.-b. Yang, Natural xanthones from Garcinia mangostana with multifunctional activities for the therapy of Alzheimer's disease, Neurochem. Res. 41 (2016) 1806–1817.
[17] Y. Wang, Z. Xia, J.-R. Xu, Y.-X. Wang, L.-N. Hou, Y. Qiu, H.-Z. Chen, α-Mangostin, a polyphenolic xanthone derivative from mangosteen, attenuates β-amyloid oligomers-induced neurotoxicity by inhibiting amyloid aggregation, Neuropharmacology 62 (2012) 871–881.
[18] G. Kolokythas, I.K. Kostakis, N. Pouli, P. Marakos, A.-L. Skaltsounis, H. Pratsinis, Design and synthesis of some new pyranoxanthenone aminoderivatives with cytotoxic activity, Bioorg. Med. Chem. Lett. 12 (2002) 1443–1446.
[19] J. Negi, V. Bisht, P. Singh, M. Rawat, G. Joshi, Naturally occurring xanthones: Chemistry and biology, J. Appl. Chem. 2013 (2013).
[20] H. Zou, J.-J. Koh, J. Li, S. Qiu, T.T. Aung, H. Lin, R. Lakshminarayanan, X. Dai, C. Tang, F.H. Lim, Design and synthesis of amphiphilic xanthone-based, membrane-targeting antimicrobials with improved membrane selectivity, J. Med. Chem. 56 (2013) 2359–2373.
[21] J.-J. Koh, S. Qiu, H. Zou, R. Lakshminarayanan, J. Li, X. Zhou, C. Tang, P. Saraswathi, C. Verma, D.T. Tan, Rapid bactericidal action of alpha-mangostin against MRSA as an outcome of membrane targeting, Biochim. Biophys. Acta (BBA)-Biomembr. 1828 (2013) 834–844.
[22] J.-J. Koh, H. Zou, S. Lin, H. Lin, R.T. Soh, F.H. Lim, W.L. Koh, J. Li, R. Lakshminarayanan, C. Verma, Nonpeptidic amphiphilic xanthone derivatives: structure–activity relationship and membrane-targeting properties, J. Med. Chem. 59 (2015) 171–193.
[23] V. Peres, T.J. Nagem, F.F. de Oliveira, Tetraoxygenated naturally occurring xanthones, Phytochemistry 55 (2000) 683–710.
[24] M. Sierra, L. Alarcón, D. Gerbino, V. Pedroni, F. Buffo, M. Morini, Effects of hydroxy-xanthones on dipalmitoylphosphatidylcholine lipid bilayers: a theoretical and experimental study, Chem. Phys. Lipids 206 (August 2017) 1–8.
[25] E. Kotova, T. Rokitskaya, Y. Antonenko, Two phases of gramicidin photoinactivation in bilayer lipid membranes in the presence of a photosensitizer, Membr. Cell Biol. 13 (2000) 411–420.
[26] D.S. Pellosi, V.R. Batistela, V.R.D. Souza, I.S. Scarminio, W. Caetano, N. Hioka, Evaluation of the Photodynamic Activity of Xanthene Dyes on *Artemia salina* Described by Chemometric Approaches, Anais da Academia Brasileira de Ciências, 85 (2013), pp. 1267–1274.
[27] V. Sokolov, V. Chernyĭ, V. Markin, Measurements of the potential difference during adsorption of phloretin and fluorescein on the surface of lipid membranes using the method of inner field compensation, Biofizika 29 (1984) 424–429.
[28] P. Grover, G. Shah, R. Shah, Xanthones. Part IV. A new synthesis of hydroxyxanthones and hydroxybenzophenones, J. Chem. Soc. Resumed (1955) 3982–3985.
[29] R. MacDonald, S. Simon, Lipid monolayer states and their relationships to bilayers, Proc. Natl. Acad. Sci. 84 (1987) 4089–4093.
[30] M.D.C. Luzardo, G. Peltzer, E. Disalvo, Surface potential of lipid interfaces formed by mixtures of phosphatidylcholine of different chain lengths, Langmuir 14 (1998) 5858–5862.
[31] F. Lairion, E.A. Disalvo, Effect of dipole potential variations on the surface charge potential of lipid membranes, J. Phys. Chem. B 113 (2009) 1607–1614.
[32] A.S. Rosa, A.C. Cutro, M.A. Frias, E.A. Disalvo, Interaction of phenylalanine with DPPC model membranes: more than a hydrophobic interaction, J. Phys. Chem. B 119 (2015) 15844–15847.
[33] W.F. Wolkers, H. Oldenhof, B. Glasmacher, Dehydrating phospholipid vesicles measured in real-time using ATR Fourier transform infrared spectroscopy, Cryobiology 61 (2010) 108–114.
[34] D. Case, T. Darden, T. Cheatham III, C. Simmerling, J. Wang, R. Duke, R. Luo, R. Walker, W. Zhang, K. Merz, AMBER 12, University of California, San Francisco, San Francisco, CA, 2012 (There is no corresponding record for this reference).
[35] Å.A. Skjevik, B.D. Madej, R.C. Walker, K. Teigen, LIPID11: a modular framework for LIPID simulations using amber, J. Phys. Chem. B 116 (2012) 11124–11136.
[36] W.L. Jorgensen, J. Chandrasekhar, J.D. Madura, R.W. Impey, M.L. Klein, Comparison of simple potential functions for simulating liquid water, J. Chem. Phys. 79 (1983) 926–935.
[37] M.W. Mahoney, W.L. Jorgensen, A five-site model for liquid water and the reproduction of the density anomaly by rigid, nonpolarizable potential functions, J. Chem. Phys. 112 (2000) 8910–8922.
[38] J.-P. Hansen, I.R. McDonald, Theory of Simple Liquids: With Applications to Soft Matter, Academic Press, 2013.
[39] F.M. Harris, K.B. Best, J.D. Bell, Use of laurdan fluorescence intensity and polarization to distinguish between changes in membrane fluidity and phospholipid order, Biochim. Biophys. Acta (BBA)-Biomembr. 1565 (2002) 123–128.
[40] T. Parasassi, M. Di Stefano, M. Loiero, G. Ravagnan, E. Gratton, Influence of cholesterol on phospholipid bilayers phase domains as detected by Laurdan fluorescence, Biophys. J. 66 (1994) 120–132.
[41] J.R. Lakowicz, Principles of Fluorescence Spectroscopy, Springer, US, New York, 2006.
[42] J.D. Nickels, J. Katsaras, Water and Lipid Bilayers, Springer, Membrane Hydration, 2015, pp. 45–67.
[43] H. Brockman, Dipole potential of lipid membranes, Chem. Phys. Lipids 73 (1994) 57–79.
[44] T. Parasassi, E.K. Krasnowska, L. Bagatolli, E. Gratton, Laurdan and Prodan as polarity-sensitive fluorescent membrane probes, J. Fluoresc. 8 (1998) 365–373.
[45] L.A. Bagatoll, T. Parasassi, G.D. Fidelio, E. Gratton, A model for the interaction of 6-Lauroyl-2-(N, N-dimethylamino) naphthalene with lipid environments: implications for spectral properties, Photochem. Photobiol. 70 (1999) 557–564.
[46] T. Parasassi, G. Ravagnan, R.M. Rusch, E. Gratton, Modulation and dynamics of phase properties in phospholipid mixtures detected by Laurdan fluorescence, Photochem. Photobiol. 57 (1993) 403–410.
[47] P. Jurkiewicz, A. Olżyńska, M. Langner, M. Hof, Headgroup hydration and mobility of DOTAP/DOPC bilayers: a fluorescence solvent relaxation study, Langmuir 22 (2006) 8741–8749.
[48] A. Samanta, R. Fessenden, Excited state dipole moment of PRODAN as determined from transient dielectric loss measurements, J. Phys. Chem. A 104 (2000) 8972–8975.
[49] H. Almaleck, G.J. Gordillo, A. Disalvo, Water defects induced by expansion and electrical fields in DMPC and DMPE monolayers: contribution of hydration and confined water, Colloids Surf. B: Biointerfaces 102 (2013) 871–878.
[50] M.L. Berkowitz, R. Vácha, Aqueous solutions at the interface with phospholipid bilayers, Acc. Chem. Res. 45 (2011) 74–82.
[51] W. Rawicz, B. Smith, T. McIntosh, S. Simon, E. Evans, Elasticity, strength, and water permeability of bilayers that contain raft microdomain-forming lipids, Biophys. J. 94 (2008) 4725–4736.
[52] L. Frias Mde, E.A. Disalvo, Configuration of carbonyl groups at the lipid interphases of different topological arrangements of lipid dispersions, Langmuir 25 (2009) 8187–8191.
[53] Z. Arsov, Long-Range Lipid-Water Interaction as Observed by ATR-FTIR Spectroscopy, Springer, Membrane Hydration, 2015, pp. 127–159.
[54] D.A. Mannock, T.J. McIntosh, X. Jiang, D.F. Covey, R.N. McElhaney, Effects of natural and enantiomeric cholesterol on the thermotropic phase behavior and structure of egg sphingomyelin bilayer membranes, Biophys. J. 84 (2003) 1038–1046.
[55] T.R. Lucas, B.A. Bauer, J.E. Davis, S. Patel, Molecular dynamics simulation of hydrated DPPC monolayers using charge equilibration force fields, J. Comput. Chem. 33 (2012) 141–152.